Wurtzite-type CoO-nanocrystals in ultrathin ZnCoO films

Principal publication and authors
H.L. Meyerheim (a), C. Tusche (a), A. Ernst (a), S. Ostanin (a), I.V. Maznichenko (b), K. Mohseni (a), N. Jedrecy (c), J. Zegenhagen (d), J. Roy (d), I. Mertig (b), and J. Kirschner (a), *Phys. Rev. Lett.* **102**, 156102 (2009).
(a) Max-Planck-Institut f. Mikrostrukturphysik, Halle (Germany)
(b) Inst. f. Physik, Martin-Luther-Universität Halle-Wittenberg, Halle (Germany)
(c) Inst. des Nano Sciences de Paris, Univ. P. et M. Curie-Paris 6, Paris (France)
(d) ESRF

Diluted magnetic semiconductors have become a central theme in solid state research over the last decade. They offer unique possibilities to combine new spintronic applications into existing semiconductor device architectures. In spintronic systems, information storage is based on the direction of the magnetisation (up or down) of a magnetic material. Zinc oxide (ZnO) doped with 5-20 at.% Co represents a prototype example for the class of spintronic materials, in which the Co atoms substitute Zn atoms within the wurtzite structure. In the wurtzite structure each metal atom is tetrahedrally coordinated by four oxygen atoms. Several theoretical models have been proposed to explain ferromagnetism in Zn(Co)O alloys. Most recently, Dietl *et al.* [1] have suggested the presence of uncompensated spins at the surface of antiferromagnetic wurtzite-type CoO nanocrystals within the ZnO host lattice, however direct experimental evidence for this model is so far lacking. This can be attributed to the similarity of the atomic species obscuring any clear cut discrimination using scattering and microscopy techniques.

At beamline ID32 we have carried out a surface X-ray diffraction study on cobalt doped (20%) ZnO films deposited on Ag(111) using pulsed laser deposition in the thickness range of about 1 nm. A previous study [2] has shown that in the first layer adjacent to the Ag(111) surface wurtzite-type ZnO adopts the hexagonal-boron-nitride (h-BN) structure, in which the metal atom is surrounded by oxygen atoms in a threefold planar coordination.

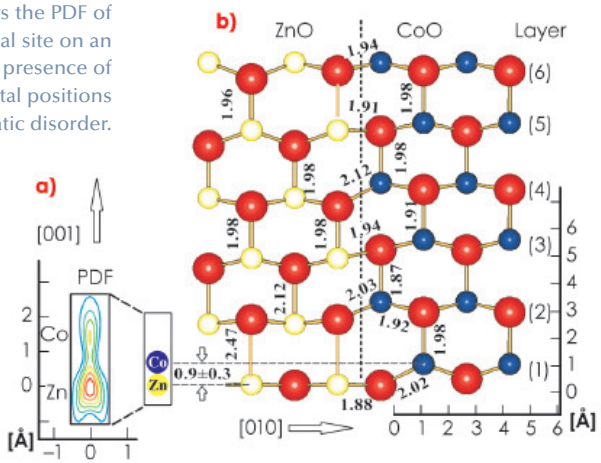

Fig. 32: Structural model for Zn(Co)O at the interface between ZnO (left) and CoO (right). Oxygen atoms are shown as large spheres. Layers are numbered from 1 to 6. Interatomic distances given in angstroms. The lower left side (a) shows the PDF of the first layer metal site on an enlarged scale. Note the presence of two distinct metal positions indicative of static disorder.

The most important result of the analysis of the X-ray data is the pronounced vertical disorder observed for the first layer metal atomic site, which diminishes in the subsequent layers. Figure 32a shows in detail the probability density function (PDF) for the first layer metal site, representing the distribution of the atomic positions. Two well defined maxima are identified separated by 0.9±0.3 Å indicating the presence of two different atomic sites. According to their relative magnitudes (3:1), the lower and upper PDF maxima can be attributed to Zn and Co, respectively. When developing a structural model, the large vertical disorder requires the separation of the ZnO and CoO phase, ruling out random alloying, since the latter would involve many metal-oxygen distances below 1.5 Å, which is incompatible with the sizes of the atoms. While ZnO adopts the planar h-BN structure, CoO crystallises in the wurtzite-phase, in which the Co atom is located several tenths of an angstrom above the plane of oxygen atoms making the two metal (oxide) species distinguishable.

This different behaviour of ZnO and CoO is supported by first principles calculations. The wurtzite to h-BN transition follows a transformation path characterised by a decreasing *c*/*a* lattice parameter ratio. The *a* lattice parameter is kept constant at the experimental value *a* = 3.27 Å and the height of the metal atom above the plane of oxygen atoms (labelled as *uc* in Figure 33) is relaxed from the value of *uc* = 0.63 Å corresponding to the WZ-phase to *uc* = 0.0 Å characterising the h-BN structure. Whereas, for ZnO we find that the transition takes place from *c* = 5.22 Å (*c*/*a* = 1.61, *uc* = 0.63 Å) to *c* = 4.21 Å (*c*/*a* = 1.3, *uc* = 0.0 Å) as shown by the solid (black) line in Figure 33. Although CoO exists in the wurtzite phase with almost the same c

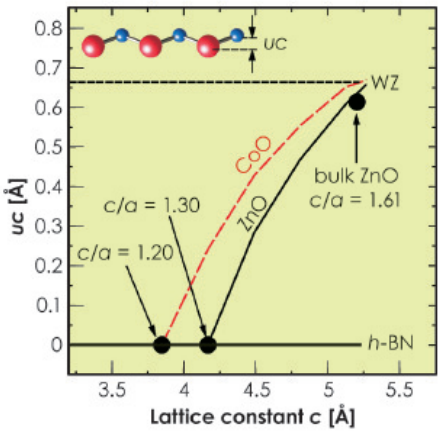

Fig. 33: Calculated *uc* vs. *c* for bulk ZnO and CoO (solid and dashed line). Parameters *uc* and *c* for wurtzite, bulk ZnO and h-BN are indicated for comparison.

lattice parameter as ZnO, the transition to the h-BN-phase requires a larger compression (c = 3.88 Å (c/a = 1.2)) directly reflecting the tendency of CoO to avoid the h-BN structure (red line in Figure 33).

In summary, our study has given evidence for the presence of CoO-nanocrystals in ZnO supporting the phase decomposition model [1].

References
[1] T. Dietl, T. Andrearczyk, A. Lipińska, M. Kiecana, M. Tay, and Y. Wu, *Phys. Rev. B* **76**, 155312 (2007).
[2] C. Tusche, H.L. Meyerheim, and J. Kirschner, *Phys. Rev. Lett.* **99**, 026102 (2007).

Squeezing single nanostructures

The spatial confinement of low-dimensional materials can influence their physical properties. The plastic regime has been investigated by nanoindentation, compression and tensile tests, whereas the *elastic* properties of individual nanoscale objects such as single nanowires were studied and contradictory results reported on the size dependence of Young's modulus. In order to study the elastic properties of individual nanostructures we combined micro X-ray diffraction (μXRD) and an *in situ* atomic force microscope (AFM, Small Infinity) which allows both topographical imaging of the sample surface and selection of a specific nanoobject. The electrochemically blunted AFM tungsten tip can be used to deform an object by applying a well-defined force. The experimental setup is presented in Figure 34a. During the application of pressure, μXRD images are simultaneously recorded giving direct access to the lattice deformation in the object. For alignment of the sample, the AFM tip, and the microfocussed X-ray beam, we employ scanning X-ray diffraction mapping (SXDM) and photocurrent imaging (PI). The focussed X-ray beam is scanned across the sample and the X-ray signal of the nanoobjects is recorded resulting in a positional 2D map of the structures. When the X-ray beam hits the AFM tip, photoelectrons are emitted inducing a photocurrent which is simultaneously recorded with the SXDM, facilitating the alignment.

In the present study, we investigated the elastic properties of individual SiGe islands, at beamline ID01. Figures 34b and 34c present an AFM image of a SiGe island and a superposition of a scanning X-ray diffraction map and a PI image, respectively. Figure 34c demonstrates the excellent alignment employing these two imaging techniques simultaneously.

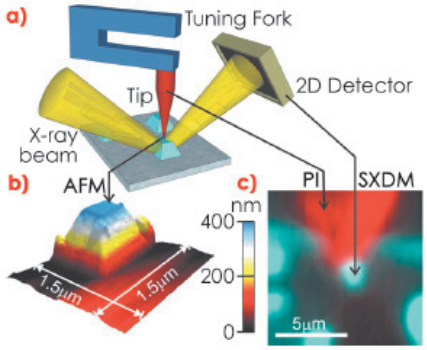

Fig. 34: a) Schematic of the experimental setup. b) Atomic force micrograph of a SiGe island. c) Superposition of simultaneous SXDM (blue) and PI (red) images.

Figure 35a shows the calculated three-dimensional reciprocal space map (3D-RSM) of a SiGe island grown on a Si(001) substrate. In the experiment, a two-dimensional detector is used, cutting through reciprocal space and thus recording only a 2D-RSM. The corresponding detector plane is represented by the semitransparent plane in Figure 35a. The related XRD pattern is displayed in Figure 35b

Principal publication and authors
T. Scheler (a), M. Rodrigues (a), T.W. Cornelius (a), C. Mocuta (a), A. Malachias (a), R. Magalhães-Paniago (a), F. Comin (a), J. Chevrier (a,b) and T.H. Metzger (a), *Appl. Phys. Lett.* **94**, 023109 (2009);
M.S. Rodrigues (a), T.W. Cornelius (a), T. Scheler (a), C. Mocuta (a), A. Malachias (a), R. Magalhães-Paniago (a), F. Comin (a), T.H. Metzger (a) and J. Chevrier (a,b), *J. Appl. Phys.* **106**, 103525 (2009).
(a) ESRF
(b) Institut Néel, CNRS-UJF, Grenoble (France)